FISEVIER

Contents lists available at ScienceDirect

Journal of Membrane Science

journal homepage: www.elsevier.com/locate/memsci



Composite hollow fiber membranes with different poly (dimethylsiloxane) intrusions into substrate for phenol removal via extractive membrane bioreactor



Chun Heng Loh^a, Yuan Zhang^a, Shuwen Goh^a, Rong Wang^{a,b,*}, Anthony G. Fane^a

- ^a Singapore Membrane Technology Centre, Nanyang Environment and Water Research Institute, Nanyang Technological University, 1 Ceantech Loop, Singapore 637141. Singapore
- ^b School of Civil and Environmental Engineering, Nanyang Technological University, 50 Nanyang Avenue, Singapore 639798, Singapore

ARTICLE INFO

Article history:
Received 7 September 2015
Received in revised form
29 November 2015
Accepted 1 December 2015
Available online 3 December 2015

Keywords:
Hollow fiber
Thin film composite membrane
Poly(dimethylsiloxane)
Phenol removal
Extractive membrane bioreactor

ABSTRACT

Due to its toxicity to ecosystem, phenol removal from industrial wastewater before discharge is a priority concern. Extractive membrane bioreactor (EMBR), a novel wastewater treatment process combining aqueous-aqueous extractive membrane process and biodegradation, has shown potential in treating phenol in wastewater. In this paper, composite hollow fiber membranes with different levels of poly (dimethylsiloxane) (PDMS) intrusion were prepared by coating a layer of PDMS on a Polyetherimide (PEI) hollow fiber substrate. Their applicability to EMBR for phenol removal was studied. The prepared membranes were characterized by microscopy and gas permeation test, and their performances were evaluated in aqueous-aqueous extractive membrane processes and EMBR process. The overall mass transfer coefficient for phenol, or k₀, was found to be significantly affected by the level of PDMS intrusion in the composite membranes. This is because the penetration of PDMS into the porous substrate results in a denser membrane structure, which consequently increases the membrane resistance. A slight penetration of PDMS into the substrate was found to be necessary for the composite membranes to achieve high k_0 while maintaining low inorganic flux across the membranes. Wilson-plot analysis suggests that membrane resistance dominated over liquid boundary layer resistances. After more than 250 h of EMBR operation, significant biofilm growth was observed on the composite membranes and the k_0 was dropped but stabilized at around 7.5×10^{-7} m/s. This k_0 was 7.5 times higher than commercial PDMS tubular membranes (without biofilm development) reported in previous studies, confirming the superiority of thin film composite membranes prepared in this work. It was also found that process optimization to control biofilm thickness is important in order to enhance phenol removal rate in EMBR. © 2015 Elsevier B.V. All rights reserved.

1. Introduction

Phenol is an organic that often presents in wastewater of many industries such as chemical, pharmaceutical, petrochemical, and paint production industries [1]. Due to its toxicity to human and ecosystem even at low concentration, phenol and phenolic compounds are listed as a priority pollutant by United States Environmental Protection Agency [2]. Therefore, it is essential to remove phenol from wastewater before discharge using reliable and economically feasible technologies. Currently, methods used for phenol removal include traditional techniques such as steam distillation [3], liquid–liquid extraction [4], adsorption [5], wet air

oxidation [6], and biodegradation [7], as well as advanced techniques such as electro-chemical oxidation [8], photo-oxidation [9] and membrane extraction [10]. Among these, biodegradation offers some advantages such as low cost and high energy efficiency. However, microorganisms can be inhibited by the toxicity of phenol at high concentration, making biodegradation suitable only for treating wastewater with low phenol concentration.

Extractive membrane bioreactor (EMBR), first proposed by Livingston, is a novel wastewater treatment process combining aqueous—aqueous extractive membrane process and biodegradation [11]. In EMBR, target organic pollutants transport through a non-porous membrane from the feed solution to the receiving solution by solution-diffusion mechanism, driven by the concentration gradient across the membrane; the organic pollutants are then biodegraded by specific microorganisms at the receiving side. Wastewater with inhibitory compounds and harsh conditions such as extreme pH and high salt concentration can be treated by

^{*} Corresponding author at: School of Civil and Environmental Engineering, Nanyang Technological University, 50 Nanyang Avenue, Singapore 639798, Singapore. E-mail address: rwang@ntu.edu.sg (R. Wang).

this process as the bioreactor is separated with the feed solution by the membrane. In addition, the ongoing biodegradation helps to maintain low (or zero) organic concentration at the receiving side, maintaining the organic concentration gradient across the membrane as the driving force.

The membranes used in EMBR should have a high organic flux while being effectively impermeable to inorganics and water. Most commonly used membrane materials for this application are silicon-based rubbers such as poly(dimethylsiloxane) (PDMS) and poly(vinylmethylsiloxane) (PVMS) [12,13]. The Si-O units that comprise the PDMS backbone make it a highly flexible polymer and thus small molecules are able to transport through the free volume of PDMS. In addition, PDMS exhibits hydrophobicity and organophilicity, making it highly permeable for organic compounds [14,15]. However, phenol transfer rate across PDMS membranes has been found to be much lower compared with those of other aromatic compounds such as toluene, benzene, and monochlorobenzene [16,17]. This is due to the relatively hydrophilic nature of phenol that causes phenol to have a lower affinity to PDMS. Therefore, membrane resistance was reported to always dominate over liquid boundary layer resistances in the case of phenol extraction [11]. In most of the previously reported studies on EMBR, commercial silicon rubber tubes which had a thickness of at least 0.2 mm were used as the membranes for phenol extraction [11,12,17]. The large thickness of silicon tubes further increased membrane resistance to phenol transfer and thus limited the feasibility of removing phenol via EMBR.

A strategy to reduce the membrane resistance to phenol transfer is to prepare thin film composite membranes, which consist of a thin PDMS film as the selective layer and a porous substrate as the mechanical support. The use of PDMS composite membranes have been reported to significantly enhance organic transfer in other organic extraction applications such as aqueous–aqueous extractive membrane process and membrane aromatic recovery system [18,19]. However, the use of composite membrane and its systematic performance study in EMBR have not been reported so far. Therefore, for the first time, this paper discusses the preparation of thin film composite hollow fiber membranes to address the issue of low phenol transfer in EMBR.

When doing coating of PDMS on a porous substrate, one issue that often arises is the intrusion of PDMS into the pores of the substrate. While PDMS intrusion may help in enhancing the adhesion between the coating layer and the substrate, it also increases the membrane resistance. It has been reported that the mass transfer resistance of a composite membrane increases linearly with the PDMS intrusion depth [20]. Therefore, PDMS intrusion is normally undesirable and hence various techniques, such as pre-wetting of substrate pores by liquid and use of highviscosity coating solution, have been employed to minimize it during coating [20,21]. In this work, PDMS was coated on Polyetherimide (PEI) hollow fiber substrate to prepare composite membranes, while membranes with different levels of PDMS intrusion were prepared for comparison. Through various characterization methods including microscopy, gas permeation test, and performance evaluation in aqueous-aqueous extractive processes, the efficiency for phenol transfer, structural integrity, longterm stability, and significance of membrane resistance/liquid boundary layer resistances of the resultant composite membranes were examined. Finally, selected membranes were subjected to EMBR operation. By carrying out the abovementioned studies, this paper aims to demonstrate the applicability of composite hollow fiber membranes to EMBR process and the importance of membrane optimization to enhance phenol removal while maintaining minimum salt and water flux.

2. Experimental

2.1. Materials and chemicals

Polyetherimide (PEI) (Ultems® 1000, M_n =12,000, GE Plastics) was used as the hollow fiber membrane material. A silicon elastomer and a curing agent were dissolved in an appropriate solvent to prepare the coating solution. Phenol (p K_a in water=9.95) was obtained from Sigma-Aldrich while NaCl, HCl (37%), and NaOH were purchased from Merck. MgSO₄·7H₂O, KH₂PO₄, KH₂PO₄, FeCl₃, CaCl₂·2H₂O, and NH₄Cl from Merck were used as the nutrients for biomedium, All the reagents were used as received. Deionized water (DI water) was produced from a Milli-Q® water purification system. High-purity gases including O₂ and N₂ were supplied by Singapore Oxygen Air Liquide (SOXAL). For experimental setups involving phenol solution, tubings and fittings made of Viton®, polytetrafluoroethylene (PTFE), or polypropylene (PP) were used to prevent phenol absorption.

2.2. Preparation of PDMS-PEI composite membranes

PEI hollow fiber membranes were prepared via dry-jet wet spinning technique as described elsewhere [22,23], and the membrane characteristics are listed in Table 1. Lab-scale hollow fiber modules were made by sealing 5 pieces of 20-cm-length hollow fibers in plastic tubing. Coating solution was then injected through the lumen side of the hollow fibers to create a PDMS layer on the PEI substrate. Different levels of PDMS intrusion were achieved on the composite membranes by changing coating conditions. The codes of prepared composite membranes (CI, PI-a, PI-b, and PI-c) were listed in Table 2.

2.3. Membrane characterizations

The cross-sectional and surface morphologies of hollow fiber membranes were observed using a field emission scanning electron microscope (FESEM) (JSM-7600F, JEOL). The membranes were broken in liquid nitrogen and sputtered with platinum prior to the test. The PDMS intrusion in the composite membranes was characterized by examining the distribution of silicon element at different locations along the membrane cross-section using Energy-dispersive X-ray spectroscopy (EDX) (coupled with FESEM). The contact angle of hollow fibers was measured based on the procedure mentioned in previous studies [24,25]. The contact angle for shell surface was measured by sealing the lumen using epoxy glue.

2.4. Gas permeation test

 O_2/N_2 selectivity can serve as an indicator to check if the composite membranes are defect free. The setup for gas permeation test was similar to that described in the literature [26]. Feed gas flowed through the lumen of hollow fibers while the gas flow rate (100 mL/min) was controlled by a mass flow controller (Model 32907-63, Cole Parmer). The feed pressure was adjusted to 0.5 bar

Table 1Characteristics of PEI hollow fiber substrate.

Parameter	Value	
OD (μm)	1020 ± 8	
ID (μm)	740 ± 9	
Thickness (µm)	140 ± 4	
Pore size (µm)	$\textbf{0.05} \pm \textbf{0.01}$	
Overall Porosity (%)	82 ± 1	
Contact angle (deg)	77 ± 3	

Table 2Prepared composite membranes with different levels of PDMS intrusion.

Code of prepared membrane	Level of PDMS intrusion	Remarks
CI PI-a PI-b PI-c	Complete intrusion Partial intrusion Partial intrusion Partial intrusion	↓increasing coating flow velocity

using a back pressure regulator. The permeate flow rate was measured at the shell side of hollow fibers by a bubble flow meter (Defender 510, Bios International). The gas permeances for O_2 and N_2 and the O_2/N_2 selectivity were calculated based on the following equations:

$$\frac{P}{L} = \frac{Q}{A\Delta P} \tag{1}$$

$$\alpha = \frac{(P/L)_{0_2}}{(P/L)_{N_2}} \tag{2}$$

where P/L is the gas permeance (GPU or $10^{-6} \, \mathrm{cm}^3$ (STP)/ (cm² s cm Hg)); Q the permeate gas flow rate (cm³/s); A the membrane surface area (cm²); ΔP the transmembrane pressure (cm Hg); α the O_2/N_2 selectivity.

2.5. Aqueous-aqueous extractive processes

Fig. 1 shows the crossflow aqueous–aqueous extractive setup used for phenol removal using the prepared composite membranes. A steady state can be achieved after a certain period of time by applying a constant purge flow of DI water through the receiving solution. The efficiency of phenol transfer across a composite membrane was characterized by the overall mass transfer coefficient, which is independent of concentration driving force [16]. The overall mass transfer coefficient can be determined from the following mass balance equation, which shows that the rate of change of phenol in receiving solution equals to the difference between the phenol flux across the membrane and the phenol loss through the purging:

$$V_r \frac{dC_r}{dt} = k_0 A (C_f - C_r) - Q C_r \tag{3}$$

where V_r is the volume of receiving solution; C_f and C_r the phenol concentration at feed side and receiving side, respectively (g/m^3) ; dC_r/dt the rate of change of receiving side phenol concentration $(g/m^3 s)$, which becomes zero at steady state; k_0 the overall mass

transfer coefficient (m/s); A the membrane surface area; Q the purging flow rate (m^3/s).

Four sets of aqueous–aqueous extractive tests were carried out for different purposes:

- (a) Effect of pH on k₀ was studied using feed solutions containing 1 g/L phenol and 50 g/L sodium chloride. The pH of the feed solutions, ranging from 2 to 11, was adjusted by hydrochloric acid or sodium hydroxide. A purging flow rate of 15 mL/min was applied at the receiving side to achieve a steady state within 3 h of operation. Reynolds numbers of 1000 were applied at both sides.
- (b) Effect of PDMS intrusion on k_0 was studied using feed solutions containing 1 g/L phenol and 50 g/L sodium chloride without pH adjustment (pH \approx 6). Reynolds numbers of 1000 were applied at both sides while the purging flow rate was 15 mL/min.
- (c) Wilson-plot method, which has been described in the literature [16,27], was utilized to examine the relative influence of membrane resistance and liquid boundary layer resistance. The experiment conditions were same as (b) but the Reynolds numbers were changed from 400 to 2000 at one side while fixed at the other side.
- (d) To examine if the prepared composite hollow fibers were defect-free and remained stable over long operating period under harsh conditions (i.e., high phenol concentration), a solution containing 2 g/L phenol and 50 g/L sodium chloride was used as the feed. The phenol concentration was maintained by periodically adding concentrated saline phenol to the solution. Theoretically, membranes with defect-free PDMS layer should show no inorganic flux across the membrane. Therefore, as an indicator for membrane defect detection, NaCl flux was monitored by measuring the sodium concentration in the receiving solution using inductively coupled plasma optical emission spectrometry (ICP-OES) (Optima 8000, Perkin Elmer). No purging flow was applied in this set of experiment to avoid significant dilution of sodium chloride concentration in the receiving solution. Reynolds numbers of 1000 were applied at both sides.

2.6. Extractive membrane bioreactor process

The set up of crossflow extractive membrane bioreactor (CF-EMBR) was similar to that of aqueous-aqueous extractive tests as shown in Fig. 1, except that DI water was replaced by biomedium as the receiving solution and no purging flow was applied. Hollow fiber module information is as per stated in Section 2.2. Sludge, which had been acclimated to 750 ppm phenol, was inoculated into the bioreactor at the start of the experiment. To provide

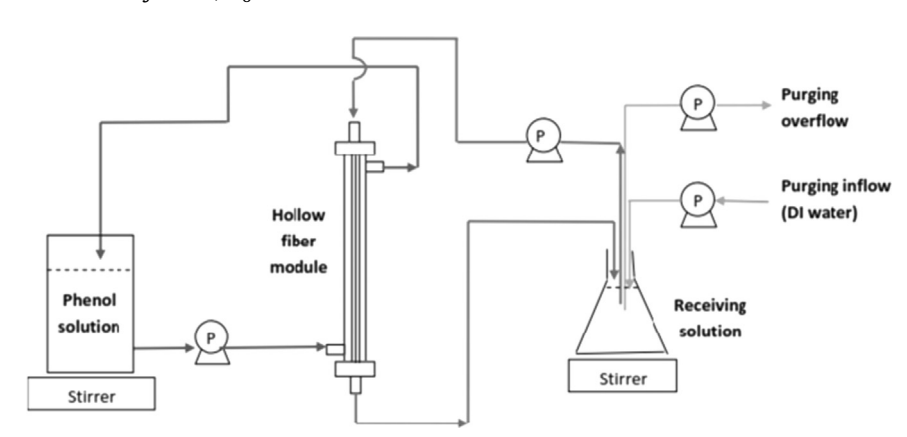


Fig. 1. Experiment setup for aqueous-aqueous extractive process.

essential inorganic nutrients to the bioreactor, a concentrated inorganic feed comprising of 20 g/L MgSO₄·7H₂O, 84 g/L KH₂PO₄, 75 g/L KH₂PO₄, 0.1 g/L FeCl₃, 10 g/L CaCl₂ · 2H₂O, and 120 g/L NH₄Cl were dosed at a rate of 20 mL/d to the bioreactor. The only source of carbon for the bioreactor was the phenol diffusing across the composite membranes from the feed solution. The feed solution used in this series of experiment was 1 g/L phenol with 50 g/L sodium chloride; the phenol concentration was maintained by periodically adding concentrated saline phenol to the solution. The Reynolds numbers for the feed and receiving sides were both around 1000. Feed and bioreactor volumes were 1 L and 4 L, respectively. pH in bioreactor was maintained at 6.9 ± 0.4 throughout the experiment while conductivity remained at 4.7 ± 0.4 mS/ cm, indicating negligible salt flux from the feed solution. Analysis of biomedium (eg. total suspended solids (TSS)) and membrane autopsy methods were mentioned in a previous study [28].

Since the phenol concentration at receiving side would be undetectable due to complete biodegradation of phenol, Eq. (3) was modified to consider the rate of change of feed side phenol concentration for k_0 calculation:

$$V_f \frac{dC_f}{dt} = k_0 A (C_f - C_r) \tag{4}$$

Since $C_r \approx 0$, $(C_f - C_r) \approx C_f$ the daily k_0 can be determined from the following equation, obtaining by integrating Eq. (4):

$$k_0 = \frac{V_f}{At} \ln \frac{C_f^t}{C_f^0} \tag{5}$$

where C_f^t and C_f^0 are the feed phenol concentrations at time t and time 0, respectively.

3. Results and discussion

3.1. Membrane characterizations

3.1.1. Morphology of PEI substrate and composite membranes

Fig. 2 shows the surface and cross-sectional morphologies of the PEI hollow fiber membranes used in this work. Both the shell and lumen surface appeared to be highly porous while the cross-section exhibited needle-like structure, indicating that the phase inversion process was dominated by instantaneous demixing during membrane formation [24]. The needle-like macrovoids are favorable as they provide low tortuosity to permeate transport without compromising too much of mechanical strength. As listed in Table 1, the membrane also showed a high overall porosity of 82%. The high porosity and low tortuosity of the membrane make it a suitable candidate as the substrate for preparing PDMS-PEI composite membranes.

The morphology near the lumen side of PDMS-coated hollow fibers is depicted in Fig. 3. A uniform layer of PDMS coating layer can be observed on top of all the composite membranes (Fig. 3a–d). The PDMS thickness on top of substrate was 1–5 μ m for membrane CI while that for membranes PI-a, PI-b, and PI-c were 0.5–2 μ m. The lumen surface for all the composite membranes (not shown in figure) was smooth and no surface pore was observed, suggesting that the surface was fully covered by PDMS.

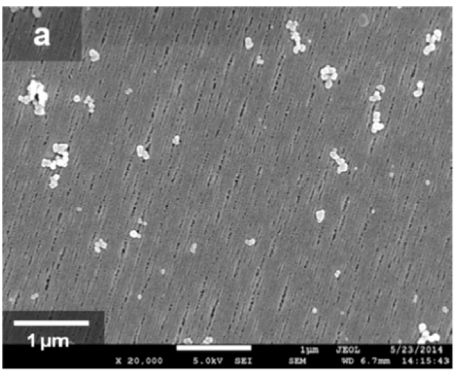
3.1.2. PDMS distribution across the composite membranes

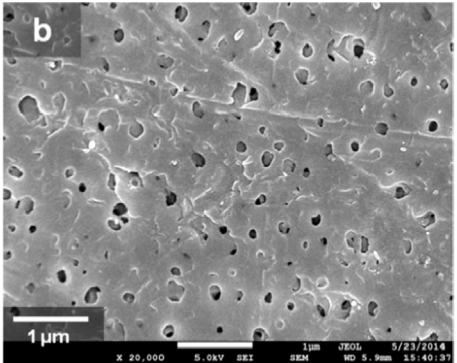
Elemental analysis for prepared composite hollow fibers was carried out using EDX. For the coating layer, elements detected include carbon, oxygen, and silicon, which are in accordance to the chemical formula of PDMS. Since PEI substrate does not contain silicon element, distribution of PDMS across the membranes can be characterized by the presence of silicon. As shown in Fig. 4, silicon can be detected across the whole cross section for membrane CI. This indicates that coating occurred not only on membrane surface but also in the substrate matrix, forming composite hollow fibers with complete PDMS intrusion. For membranes PI-a, PI-b, and PI-c, silicon can only be detected in the region of substrates within 2-um distance from PDMS coating layer, no silicon was detected in the rest part of the substrates. In other words, these membranes exhibited partial PDMS intrusion. The PDMS intrusion into the substrate of membrane CI can also be observed in Fig. 3a, which shows a much denser substrate structure compared with the composite membranes with partial PDMS intrusion (Fig. 3b-d).

In Fig. 4, it can be observed that the silicon content near the shell side (location F) is relatively high despite that the coating was employed at the lumen side. In fact, the PDMS amount near the shell side of membrane CI is so high that it almost fully covered the shell surface, making the original porous structure of uncoated shell surface no longer visible after coating, as shown in Fig. 3e. In contrast, the shell surface of composite membranes with partial PDMS intrusion still remained porous, as shown in Fig. 3f.

3.1.3. O_2/N_2 selectivity

To detect possible defects in the prepared composite hollow fibers, O_2/N_2 selectivity for the membranes was compared with that for PDMS. PDMS was reported to have high gas permeability and good selectivity: Markel et al. reported that the intrinsic O_2/N_2 selectivity for PDMS was 2, while Li et al. observed values between 1.9 and 2.4 for their defect-free PDMS composite hollow fiber membranes [14,20]. The higher O_2 permeance across PDMS compared with N_2 is mainly due to a higher solubility of O_2 in PDMS [14]. Table 3 lists the gas permeance and O_2/N_2 selectivity for composite hollow fiber membranes prepared in this work. It can be seen that the O_2/N_2 selectivity for the prepared composite membranes was about 2.2–2.4, which agrees well with the values





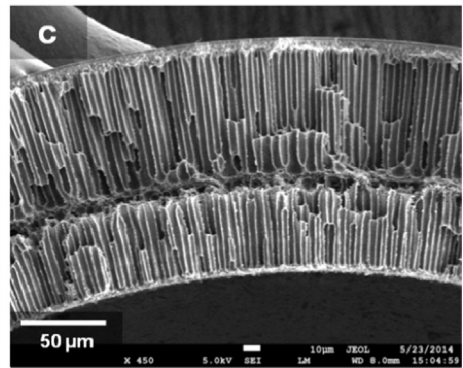


Fig. 2. Surface and cross-sectional morphologies of PEI hollow fiber substrate: (a) lumen surface, (b) shell surface, and (c) cross section.

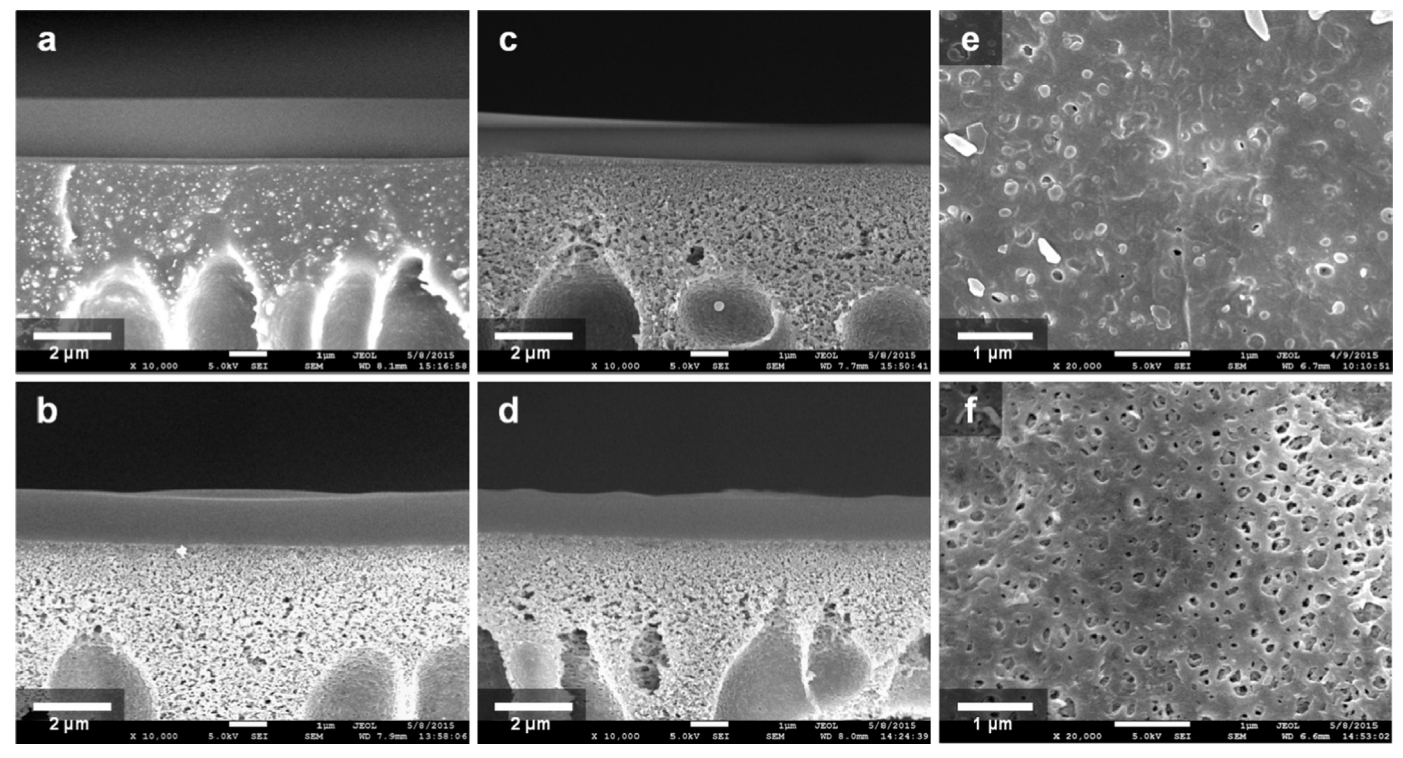


Fig. 3. Cross section showing PDMS coating layer (a to d) and shell surface (e and f) for composite membranes: (a) CI, (b) PI-a, (c) PI-b, (d) PI-c, (e) CI, and (f) PI-c.

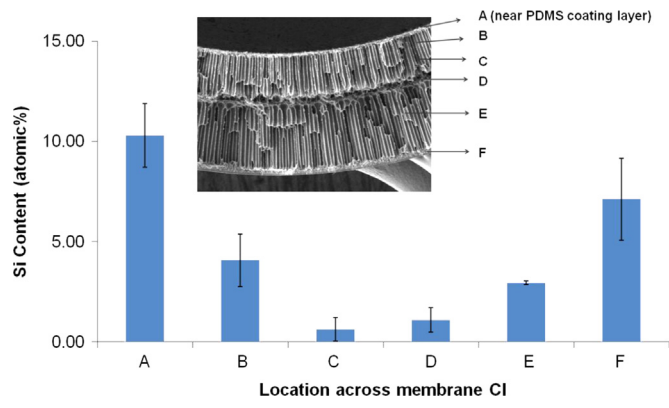


Fig. 4. Distribution of silicon element across the cross section of membrane Cl.

Table 3Gas transport properties of composite hollow fiber membranes.

	Membrane	O ₂ permeance (GPU)	N ₂ Permeance (GPU)	O ₂ /N ₂ selectivity
•	CI PI-a PI-b PI-c	83 ± 7 243 ± 6 240 ± 1 248 ± 7	38 ± 5 104 ± 7 101 ± 1 108 ± 1	2.2 2.3 2.4 2.3

reported in literature, indicating that the PDMS coating layer was defect-free for all the prepared hollow fibers. On the other hand, the O_2 and N_2 permeances for membrane CI were significantly lower than those for the other membranes, suggesting that membrane with complete PDMS intrusion exhibited a higher mass transfer resistance. This is because the gases need to transport through a thicker PDMS layer due to the penetration of PDMS into the porous substrate. It can also be observed that a change in coating flow velocity did not significantly affect the membrane

resistance, as evidenced by the similar gas permeances for membranes PI-a, PI-b, and PI-c.

3.2. Aqueous-aqueous extractive process

3.2.1. Effect of pH on phenol mass transfer

Being a weak acid, a portion of phenol will dissociate into its ionic state (i.e., $HA \leftrightarrow H^+ + A^-$). The fraction of phenol undergoing dissociation is pH dependent and can be theoretically determined based on its p K_a . In Eq. (3), the phenol concentrations C_f and C_r are total concentration including both the undissociated and the ionic phenol concentrations ($C=[HA]+[A^-]$). While the total phenol concentration does not vary with pH, [HA] will vary with pH. Therefore, the observed k_0 determined based on Eq. (3) might differ with varying pH.

To investigate the effect of pH on the observed k_0 , selected composite hollow fibers were operated using feeds with pH ranged from 2 to 11. Fig. 5 shows the effect of feed pH on the observed k_0 for membrane CI. It can be seen that the observed k_0 maintained at around 14×10^{-7} m/s when the feed pH was increased from

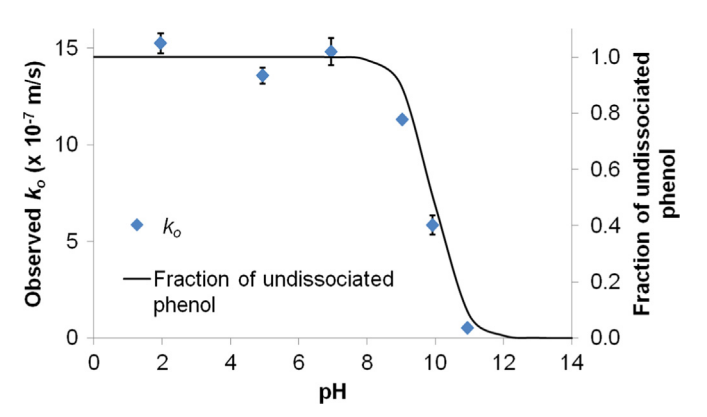


Fig. 5. Effect of feed pH on k_0 for membrane CI compared with the theoretical fraction of undissociated phenol.

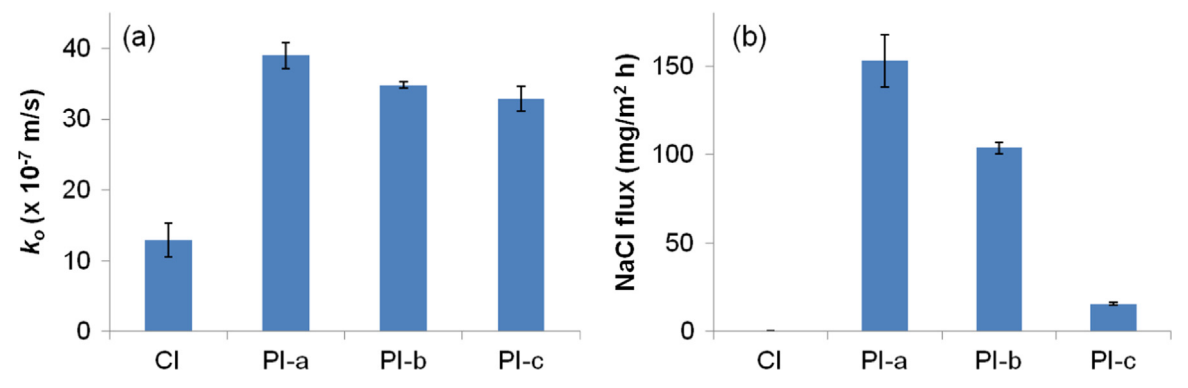


Fig. 6. (a) k_0 and (b) salt flux of composite hollow fibers prepared with different levels of PDMS intrusion.

2 to 7. A sharp decrease in the k_0 was then observed when the feed pH was over 8. This change in observed k_0 over pH of feed solution agrees well with the dissociation behavior of phenol in aqueous solution as shown by the theoretical line for fraction of undissociated phenol, which is also plotted in Fig. 5. This suggests that only undissociated phenol was able to transport through the composite membrane. Since PDMS is hydrophobic and non-polar, it is reasonable that solution and diffusion of phenol through PDMS is only for its uncharged species. Therefore, feed solutions with pH 6 or below were used in the following studies in this work to ensure negligible dissociation of phenol.

3.2.2. Effects of coating conditions on k_0 and salt flux

The k_0 and salt flux of composite hollow fiber membranes with different PDMS intrusions are shown in Fig. 6. As shown in Fig. 6a, membrane CI possessed a k_0 of 13×10^{-7} m/s, an order of magnitude higher than the k_0 of commercial silicon tubing $(1 \times 10^{-7}$ m/s) and comparable to k_0 of commercial PDMS-PES composite membrane $(12 \times 10^{-7}$ m/s) reported previously [16,18]. The significantly higher k_0 of membrane CI compared with silicon tubing can be attributed to the much thinner PDMS selective layer of composite membrane, which significantly reduces membrane resistance. In addition, no salt flux was detected for membrane CI as shown in Fig. 6b, indicating that the membrane remained defect-free and allowed only phenol diffusion across the membrane during the extractive process.

The k_0 was observed to be significantly enhanced to $39 \times 10^{-7} \, \text{m/s}$ for membrane PI-a, which exhibited only slight PDMS intrusion as discussed in Section 3.1.2. Apparently, PDMS intrusion into the substrate should be minimized to reduce membrane resistance. However, salt flux of about 150 mg/m² h was detected for the membrane, suggesting that there was also an increase in water diffusion across the membrane. Considering that all the prepared composite membranes exhibited defect-free coating layer as evidenced by their O_2/N_2 selectivity (Section 3.1.3), the increase in water flux for membrane PI-a might be attributed to swelling of PDMS by phenol absorption. It has been reported that PDMS swelling would induce shear stress at the interface between the skin layer and the substrate, affecting the structural stability of the composite membranes [29,30]. The integrity between the coating layer and the substrate is believed to be weaker for membrane PI-a since it has very little PDMS intrusion into the substrate compared with membrane CI. As a result, an increased salt flux was observed for membrane PI-a.

To enhance integrity between the PDMS coating layer and the substrate while still preventing severe PDMS intrusion, a slightly enhanced penetration of coating solution into the substrate might be beneficial. This could be achieved by increasing the coating flow velocity, which would generate a higher pressure in the lumen of hollow fibers. By comparing membranes PI-a, PI-b, and PI-c which

were prepared with increasing coating flow velocity, it can be observed that the salt flux decreased almost 90% from 153 to $16 \text{ mg/m}^2 \text{ h}$ (Fig. 6). This suggests that the integrity between the PDMS coating layer and the substrate was improved with increasing coating flow velocity, probably due to slightly enhanced PDMS intrusion. Meanwhile, the decrease in k_0 was less than 20%, revealing that the thickness of PDMS coating layer did not significantly change with coating flow velocity.

3.2.3. Analysis on membrane resistance and liquid boundary layer resistances

Wilson-plot method was employed to examine the significance of membrane resistance with respect to boundary layer resistance for the composite hollow fiber membranes. Membranes with the lowest and the highest k_0 , i.e., membranes CI and PI-a, were selected for the test. The value of exponent for the Reynolds number was taken to be 0.8 as it showed the best linear fit. The mass transfer resistance at one liquid side can be determined by the slope of Wilson plot while the intercept gives the sum of the membrane resistance and the mass transfer resistance at the other liquid side. The mass transfer resistance for the boundary layer at different Reynolds numbers and the membrane resistance can then be determined.

As shown in Fig. S1, the Wilson plots show reasonably wellfitted straight line using the data points tested within the Reynolds number value of 400–2000, indicating that the value of exponent used for the Reynolds number is reasonable for laminar flow. From these Wilson plots, mass transfer resistance at the boundary layers and the membrane resistance at different Reynolds numbers were calculated, as shown in Fig. 7. The membrane resistance for membrane CI $(7.0 \times 10^5 \text{ s/m})$ was 3 times higher than that for membrane PI-a $(2.3 \times 10^5 \text{ s/m})$. It can be seen that the membrane resistance was dominating over boundary layer resistances at Reynolds number > 500 for both membranes CI and PI-a. However, for the case of membrane PI-a, the boundary layer resistance become relatively significant compared with membrane CI due to the former's much lower membrane resistance. Nevertheless, the dominance of membrane resistance for both developed membranes at even laminar flow suggests that further increasing Reynolds number may bring limited improvement in k_0 for the aqueous-aqueous extractive process.

3.2.4. Long-term performance

To examine the stability (in terms of k_0 and salt flux variation with time) of the developed composite membranes, the membranes were continuously run in the aqueous–aqueous extractive process with feed containing high phenol concentration (2 g/L of phenol) for more than 350 h. Both membrane CI with complete PDMS intrusion and membrane PI-c with partial PDMS intrusion were selected for the long-term stability test. As shown in Fig. 8,

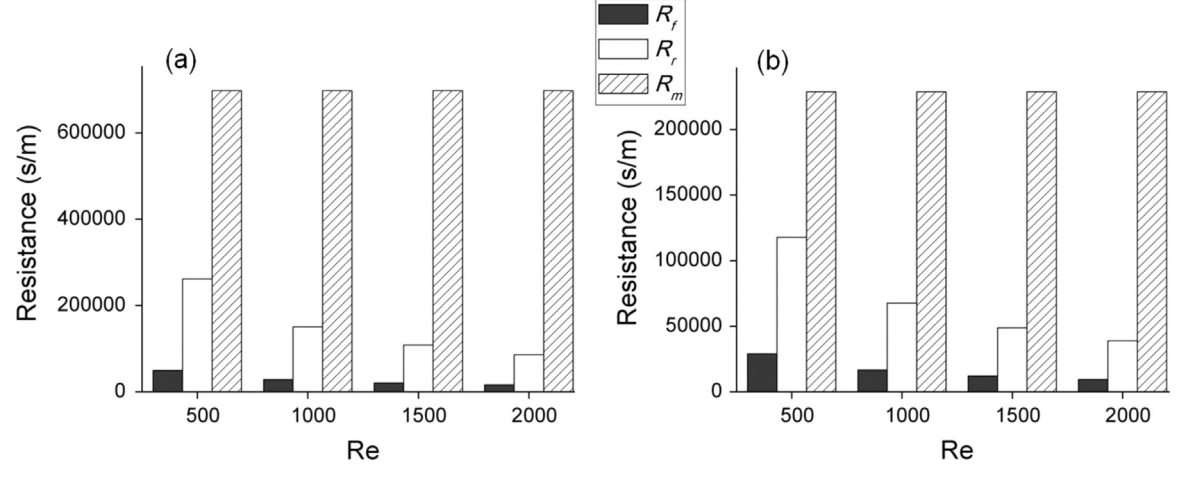


Fig. 7. Boundary layer resistance at feed side (R_f) , receiving side (R_r) , and membrane resistance (R_m) for (a) membrane CI and (b) membrane PI-a derived from Wilson plot.

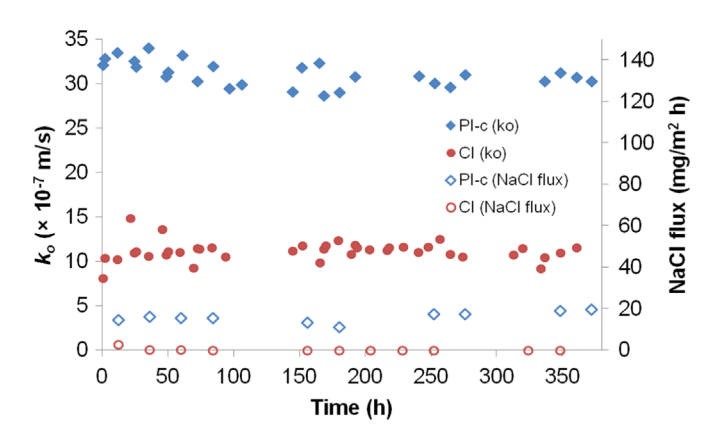


Fig. 8. Long-term performance of aqueous-aqueous extractive process for membranes CI and PI-c.

there was no significant change in k_0 over the testing period for both membranes. In addition, no salt flux was detected for membrane CI, revealing its stable structural integrity over longer period of time. Due to little PDMS intrusion compared with membrane CI as discussed in Section 3.2.2, membrane PI-c showed a salt flux of 15–18 mg/m² h. However, the salt flux remained stable over the whole operating period. This implies that the membrane integrity did not deteriorate when the membrane was in prolonged contact with phenol. The salt flux detected for membrane PI-c might not be an issue if it is not significantly high to bring impact to the EMBR performance. Therefore, both membranes CI and PI-c showed potential for EMBR application, with the former exhibited better structural integrity and the latter possessed much higher k_0 . Both membranes were selected to test their performance in EMBR process, as discussed in the following section.

3.3. Performance of composite hollow fibers in EMBR

Periodic sampling from the bioreactors showed that the phenol concentration in the bioreactor remained at zero, demonstrating that the acclimated sludge was capable of removing all phenol that had diffused from the feed solution to the receiving side. Conductivity in the bioreactor remained at 4.7 ± 0.4 mS/cm, indicating negligible impact of salt flux from the feed solution. From Fig. 9, a sharp decrease in k_0 can be observed for membrane PI-c within the first few days, while decrease in k_0 for membrane CI was less significant. The higher initial k_0 for membrane PI-c might have encouraged a faster biofilm growth on the membrane surface,

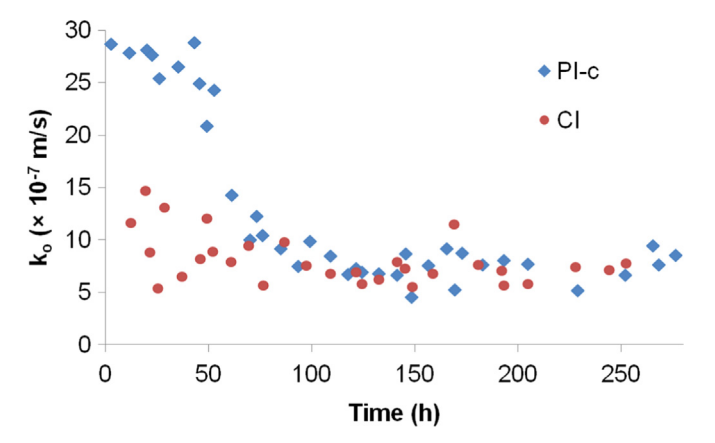


Fig. 9. EMBR performance for membranes CI and PI-c.

since the biomedium in this system received a greater amount of phenol from the feed side. As a result, despite the higher initial k_0 exhibited by membrane PI-c with partial PDMS intrusion, the stabilized k_0 at the end of the test were similar at around $7.5 \times 10^{-7} \, \text{m/s}$ for both membranes. Visual inspection of the membranes after more than 250 h of operation showed that a thick layer of biofilm had encased the hollow fibers in both cases (Fig. S2). This reveals that without process optimization to control the biofilm thickness, the thick biofilm would become the dominant mass transfer resistance in the EMBR system. Membrane autopsy showed that the amount of biomass deposited on surface of membrane PI-c was $19.3 \pm 4.5 \text{ mg TSS/cm}^2$, which was slightly higher than the $14.6 \pm 2.9 \text{ mg TSS/cm}^2$ observed on membrane CI. Again, the higher phenol loading rate due to the high k_0 at the start of the experiment may have resulted in the greater biomass growth in membrane PI-c. However, the slight difference in mg TSS/cm² did not affect the biofilm resistance significantly, as demonstrated by the similar k_0 exhibited in both modules after 250 h of operation. Nevertheless, the stabilized k_0 after more than 250 h of operation were 7.5 times higher than the k_0 exhibited by commercial PDMS tubular membranes $(1 \times 10^{-7} \text{ m/s})$ before biofilm development) in an earlier extractive membrane study [16].

Fig. 10 shows SEM images of the membranes before and after they were cleaned via ultra-sonication during membrane autopsy. Before ultra-sonication, a dense thick biofilm layer was observed (Fig. 10a and c) on the shell surface of both membranes. EDX analysis showed that the dominant elements in the biofilm were carbon and oxygen, indicating that the main component of the biofilm was organic. Ultra-sonication appears to remove most of

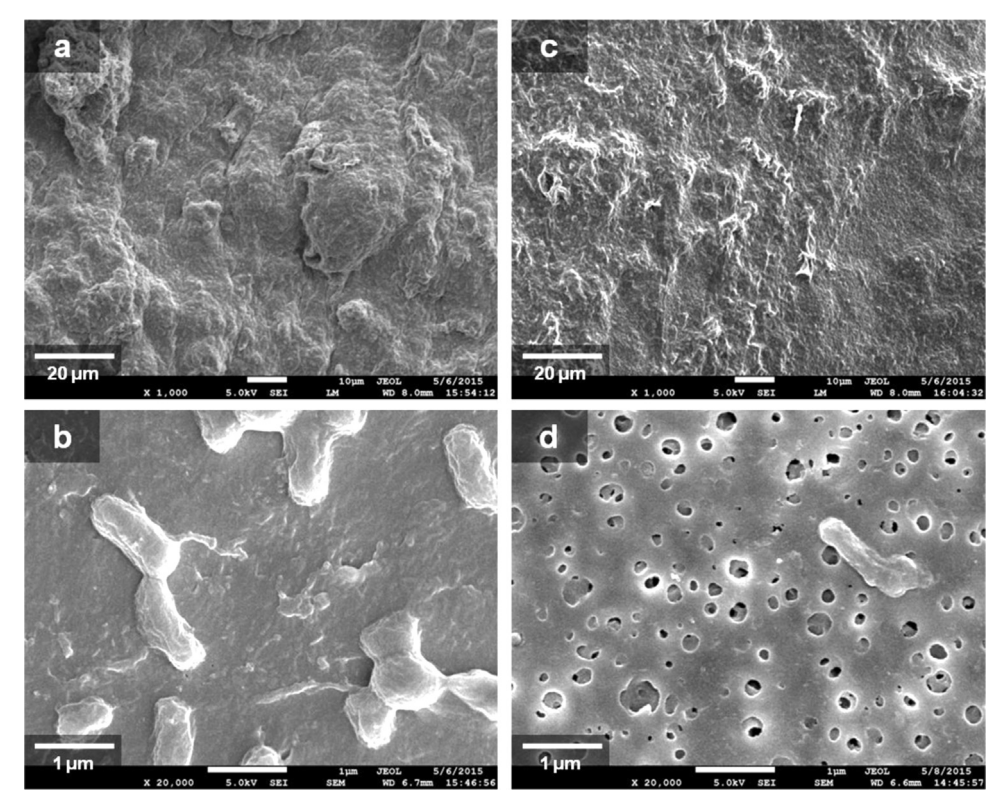


Fig. 10. SEM images of membrane shell surface after EMBR operation: CI (a) before and (b) after ultra-sonication; PI-c (c) before and (d) after ultra-sonication.

the organic and biofilm from the surface of membrane PI-c (Fig. 10d) while a dense layer of organic remains on the surface of membrane CI after ultra-sonication (Fig. 10b). As discussed in Section 3.1.2, the complete PDMS intrusion led to coverage of PDMS on the shell surface of membrane CI. In contrast, shell surface of membrane PI-c remained free of PDMS. As a result, the shell surface of membrane CI became more hydrophobic (contact angle = $126 \pm 3^{\circ}$) while that of membrane PI-c (contact angle= $79 \pm 1^{\circ}$) was relatively hydrophilic with a contact angle similar to the PEI substrate ($80 \pm 9^{\circ}$). The relatively hydrophilic shell surface of membrane PI-c might have led to weaker attractive forces between the membrane and the biofilm so the biofilm can be dislodged more easily. This could be a favorable point in terms of biofilm control; however, it is believed that a thin biofilm is still necessary to create a concentration gradient on the membrane surface. Further studies applying biofilm control strategies (eg. aeration) in the EMBR system is required to ascertain the benefits of having a more hydrophilic membrane surface for biofilm attachment.

4. Conclusions

In this work, PDMS–PEI composite hollow fiber membranes with different levels of PDMS intrusion have been prepared for removal of phenol via extractive membrane bioreactor (EMBR). Composite membranes with partial PDMS intrusion exhibited an overall mass transfer coefficient (k_0) 2.5 to 3 times higher than the composite membrane with complete PDMS intrusion. However, the former membranes suffered from weaker structural integrity and showed some salt leakage, which was mitigated by increasing the coating flow velocity. A study of the effect of feed solution pH on k_0 suggested that only undissociated phenol was allowed to transport across the prepared composite membranes. Wilson-plot analysis for the prepared membranes demonstrated that

membrane resistance is dominating over liquid boundary layer resistances while long-term performance test confirmed the stability of prepared membranes in prolonged operation.

After more than 250 h of EMBR operation, both composite membranes with complete and partial PDMS intrusions exhibited similar stabilized k_0 of around 7.5×10^{-7} m/s, despite the much higher initial k_0 for the membrane with partial PDMS intrusion. This is due to the dominance of mass transfer resistance contributed by the thick biofilm deposition, suggesting the importance of process optimization to control biofilm thickness. Nevertheless, the stabilized EMBR k_0 for the composite hollow fiber membranes was still 7.5 times higher than commercial PDMS tubular membranes (without biofilm development), confirming the superiority of thin film composite membranes.

Acknowledgments

This research grant is supported by the Singapore National Research Foundation under its Environmental & Water Technologies Strategic Research Programme and administered by the Environment & Water Industry Programme Office (EWI) of the PUB (EWI RFP 1102-IRIS-02-03). We also acknowledge funding support from the Singapore Economic Development Board to the Singapore Membrane Technology Centre. The comments and suggestions provided by Professor A. G. Livingston from Imperial College are much appreciated.

Appendix A. Supplementary material

Supplementary data associated with this article can be found in the online version at http://dx.doi.org/10.1016/j.memsci.2015.12.

References

- S. Mohammadi, A. Kargari, H. Sanaeepur, K. Abbassian, A. Najafi, E. Mofarrah, Phenol removal from industrial wastewaters: a short review, Desalination Water Treat. 53 (2014) 2215–2234.
- [2] Toxic Substances Control Act, in: USEPA (Ed.), Washington DC, 2002.
- [3] P. Barták, Pn Frnková, Lr Čáp, Determination of phenois using simultaneous steam distillation-extraction, J. Chromatogr. A 867 (2000) 281–287.
- [4] K. Abbassian, A. Kargari, T. Kaghazchi, Phenol removal from aqueous solutions by a novel industrial solvent, Chem. Eng. Commun. 202 (2014) 408–413.
- [5] G. Yang, L. Tang, G. Zeng, Y. Cai, J. Tang, Y. Pang, Y. Zhou, Y. Liu, J. Wang, S. Zhang, W. Xiong, Simultaneous removal of lead and phenol contamination from water by nitrogen-functionalized magnetic ordered mesoporous carbon, Chem. Eng. J. 259 (2015) 854–864.
- [6] K.-H. Kim, S.-K. Ihm, Heterogeneous catalytic wet air oxidation of refractory organic pollutants in industrial wastewaters: a review, J. Hazard. Mater. 186 (2011) 16–34.
- [7] H.Q. Li, H.J. Han, M.A. Du, W. Wang, Removal of phenols, thiocyanate and ammonium from coal gasification wastewater using moving bed biofilm reactor, Bioresour. Technol. 102 (2011) 4667–4673.
- [8] O. Abdelwahab, N.K. Amin, E.S.Z. El-Ashtoukhy, Electrochemical removal of phenol from oil refinery wastewater, J. Hazard. Mater. 163 (2009) 711–716.
- [9] A. Babuponnusami, K. Muthukumar, Advanced oxidation of phenol: a comparison between Fenton, electro-Fenton, sono-electro-Fenton and photo-electro-Fenton processes, Chem. Eng. J. 183 (2012) 1–9.
- [10] P. Praveen, K.C. Loh, Simultaneous extraction and biodegradation of phenol in a hollow fiber supported liquid membrane bioreactor, J. Membr. Sci. 430 (2013) 242–251.
- [11] A.G. Livingston, A novel membrane bioreactor for detoxifying industrial wastewater: I. Biodegradation of phenol in a synthetically concocted wastewater, Biotechnol. Bioeng. 41 (1993) 915–926.
- [12] E.A.C. Emanuelsson, J.P. Arcangeli, A.G. Livingston, The anoxic extractive membrane bioreactor, Water Res. 37 (2003) 1231–1238.
- [13] M. Xiao, J. Zhou, Y. Tan, A. Zhang, Y. Xia, L. Ji, Treatment of highly-concentrated phenol wastewater with an extractive membrane reactor using silicone rubber, Desalination 195 (2006) 281–293.
- [14] T.C. Merkel, V.I. Bondar, K. Nagai, B.D. Freeman, I. Pinnau, Gas sorption, diffusion, and permeation in poly(dimethylsiloxane), J. Polym. Sci. Part B: Polym. Phys. 38 (2000) 415–434.
- [15] K.-S. Chang, Y.-C. Chung, T.-H. Yang, S.J. Lue, K.-L. Tung, Y.-F. Lin, Free volume and alcohol transport properties of PDMS membranes: insights of nanostructure and interfacial affinity from molecular modeling, J. Membr. Sci. 417– 418 (2012) 119–130.
- [16] P.R. Brookes, A.G. Livingston, Aqueous-aqueous extraction of organic pollutants through tubular silicone rubber membranes, J. Membr. Sci. 104 (1995) 119–137.

- [17] S.N. Mehdizadeh, M.R. Mehrnia, K. Abdi, M.H. Sarrafzadeh, Biological treatment of toluene contaminated wastewater by Alcaligenese faecalis in an extractive membrane bioreactor; experiments and modeling, Water Sci. Technol. 64 (2011) 1239–1246.
- [18] U. Cocchini, C. Nicolella, A.G. Livingston, Countercurrent transport of organic and water molecules through thin film composite membranes in aqueous– aqueous extractive membrane processes. Part I: experimental characterisation, Chem. Eng. Sci. 57 (2002) 4087–4098.
- [19] G.R. Daisley, M.G. Dastgir, F.C. Ferreira, L.G. Peeva, A.G. Livingston, Application of thin film composite membranes to the membrane aromatic recovery system, J. Membr. Sci. 268 (2006) 20–36.
- [20] P. Li, H.Z. Chen, T.-S. Chung, The effects of substrate characteristics and prewetting agents on PAN-PDMS composite hollow fiber membranes for CO₂/N₂ and O₂/N₂ separation, J. Membr. Sci. 434 (2013) 18–25.
- [21] S. Salehi Shahrabi, H.R. Mortaheb, J. Barzin, M.R. Ehsani, Pervaporative performance of a PDMS/blended PES composite membrane for removal of toluene from water, Desalination 287 (2012) 281–289.
- [22] Y. Zhang, R. Wang, Fabrication of novel polyetherimide-fluorinated silica organic-inorganic composite hollow fiber membranes intended for membrane contactor application, J. Membr. Sci. 443 (2013) 170–180.
- [23] L. Setiawan, L. Shi, W.B. Krantz, R. Wang, Explorations of delamination and irregular structure in poly(amide-imide)-polyethersulfone dual layer hollow fiber membranes, J. Membr. Sci. 423–424 (2012) 73–84.
- [24] C.H. Loh, R. Wang, Fabrication of PVDF hollow fiber membranes: Effects of low-concentration Pluronic and spinning conditions, J. Membr. Sci. 466 (2014) 130–141.
- [25] W. Fang, L. Shi, R. Wang, Interfacially polymerized composite nanofiltration hollow fiber membranes for low-pressure water softening, J. Membr. Sci. 430 (2013) 129–139.
- [26] M. Sadrzadeh, M. Amirilargani, K. Shahidi, T. Mohammadi, Pure and mixed gas permeation through a composite polydimethylsiloxane membrane, Polym. Adv. Technol. 22 (2011) 586–597.
- [27] F. Korminouri, M. Rahbari-Sisakht, T. Matsuura, A.F. Ismail, Surface modification of polysulfone hollow fiber membrane spun under different air-gap lengths for carbon dioxide absorption in membrane contactor system, Chem. Eng. J. 264 (2015) 453–461.
- [28] S. Coh, J. Zhang, Y. Liu, A.G. Fane, Fouling and wetting in membrane distillation (MD) and MD-bioreactor (MDBR) for wastewater reclamation, Desalination 323 (2013) 39–47.
- [29] W. Wei, S. Xia, G. Liu, X. Dong, W. Jin, N. Xu, Effects of polydimethylsiloxane (PDMS) molecular weight on performance of PDMS/ceramic composite membranes, J. Membr. Sci. 375 (2011) 334–344.
- [30] P. Shao, R.Y.M. Huang, X. Feng, W. Anderson, R. Pal, C.M. Burns, Composite membranes with an integrated skin layer: preparation, structural characteristics and pervaporation performance, J. Membr. Sci. 254 (2005) 1–11.